Stabilization of metastable phases in hafnia owing to surface energy effects

Rohit Batra, Huan Doan Tran, and Rampi Ramprasad

Citation: Applied Physics Letters **108**, 172902 (2016); doi: 10.1063/1.4947490
View online: http://dx.doi.org/10.1063/1.4947490
View Table of Contents: http://scitation.aip.org/content/aip/journal/apl/108/17?ver=pdfcov
Published by the AIP Publishing

Stabilization of metastable phases in hafnia owing to surface energy effects

Rohit Batra, Huan Doan Tran, and Rampi Ramprasad[a)]
Department of Materials Science and Engineering, University of Connecticut, Storrs, Connecticut 06269, USA

(Received 1 February 2016; accepted 8 April 2016; published online 26 April 2016)

The recent empirical observation of ferroelectricity in hafnia is rather surprising since all of its known ground-state phases are nonpolar. In this letter, we show that finite size effects, relevant under experimental conditions, may themselves lead to this unexpected phenomenon due to stabilization of metastable polar phase(s). Using surface energies computed from first principles, we determine the thermodynamic stability of a parallelepiped shaped particle constructed from various low energy nonpolar and polar phases of hafnia. We find that at small dimensions, surface effects may stabilize either one of the polar phases or the nonpolar tetragonal phase (the parent phase of the polar phases), suggesting a possible explanation of the ferroelectric behavior observed in pure hafnia films. These results also explain the stabilization of the metastable tetragonal phase in nanoparticles of zirconia, the twin oxide of hafnia. While a comprehensive understanding of the origins of ferroelectricity in hafnia will require inclusion of other relevant factors (such as strain and dopants), this work highlights the importance of finite size effects as a possible key factor. *Published by AIP Publishing.*
[http://dx.doi.org/10.1063/1.4947490]

Pure and doped hafnia (HfO_2) thin films have recently garnered significant scientific interest because of their ability to produce promising ferroelectric (FE) behavior, making them strong prospects for future non-volatile storage and FE field effect transistor applications.[1,2] At first, the experimental observation of the FE behavior in hafnia films was surprising as the commonly known structural phases of hafnia, namely, the equilibrium monoclinic (M) $P2_1/c$ and the high temperature tetragonal (T) $P4_2/nmc$ phases are centrosymmetric, and thus nonpolar.[3] Several recent glancing incident X-ray diffraction and scanning transmission electron microscopy studies on hafnia films attributed the FE behavior to the presence of the polar orthorhombic (O1) $Pca2_1$ phase.[4,5] Furthermore, first-principles computations[6–8] identified fairly low free energy difference between the polar O1 and the known bulk equilibrium phases of hafnia over wide temperature and pressure ranges. Additionally, Huan *et al.*[6] found another competing, though higher in energy, polar orthorhombic (O2) $Pmn2_1$ phase. They further reported a shallow kinetic energy barrier between the T and the aforementioned polar phases, suggesting their possible formation from the T phase. Fig. 1 portrays the M, T, O1, and O2 phases discussed above, for unit cells oriented in an equivalent manner.

While the above studies provide insights concerning the potential FE phases in hafnia films, the primary causes of the stabilization of FE phase(s) remain unclear. Among the various factors, the most compelling appear to be (1) finite size effects due to the small grain sizes and film thickness,[9–11] (2) stresses associated with the substrate and electrodes,[1,12–14] and (3) the role of impurities and dopants (which include Si, Al, Gd, etc.).[1,15–17]

Here, we focus primarily on one aspect pertaining to finite size effects, namely, the role of surface energy in altering the energy ordering of hafnia phases (with respect to the energy ordering of those phases in the bulk environment). Indeed, in a closely related system, ZrO_2 (whose bulk ground state is also the M phase), the T phase is known to be stabilized in nanoparticles with sizes of the order of 25 nm.[10,18] Our goal is thus to determine if there is a possibility for hafnia phases other than the M phase to be stabilized purely due to finite size, or surface energy, considerations and lead to their formation in hafnia films. A phenomenological model of the total potential energy of a hafnia particle of finite dimensions, applicable to a variety of particle surface terminations, is proposed using which dimension-dependent stability diagrams are obtained. The parameters of this model are obtained from extensive converged first-principles computations based on density functional theory (DFT).[19,20] In addition to a possible explanation of the FE behavior observed in pure hafnia films,[12] quantitative guidance on the circumstances under which the T and the polar phases of hafnia may be expected to be stabilized is provided, thus extending the recent work.[11]

The total energy, E^α, of a particle made up of a material in a particular phase α and terminated by a set of surfaces k is given by

$$E^\alpha = n\epsilon^\alpha + \sum_k \sigma_k^\alpha A_k^\alpha, \tag{1}$$

where n is the total number of formula units of the material in the particle, ϵ^α is the energy per formula unit of the corresponding phase in the bulk, and A_k^α and σ_k^α are the area and the surface energy, respectively, of the surface k in phase α. For a particle with given dimensions, the phase with least E^α will be most favored. Thus, a metastable phase with higher bulk energy can become a stable phase in a finite sized particle if it has relatively low surface energy contributions.

We note that the above model equation is valid only if the material does not undergo reconstruction near the surfaces and if the edge and corner contributions to the total energy are small. Further, we simplify our discussion by restricting ourselves to a parallelepiped shaped material particle that has three pairs of non-parallel surfaces.

a)rampi.ramprasad@uconn.edu. URL: http://rampi.ims.uconn.edu/

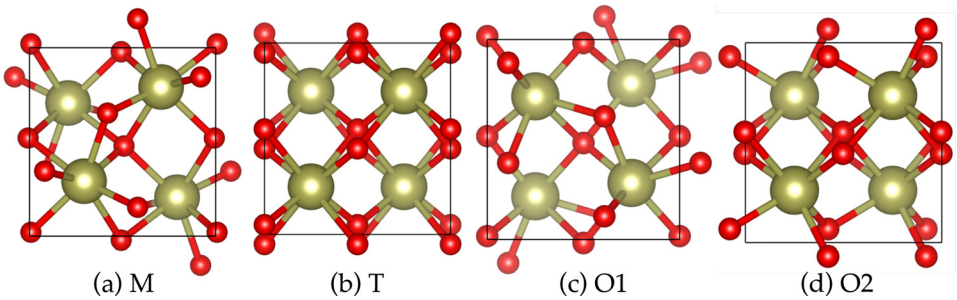

FIG. 1. (100) projections of equivalent supercells of hafnia in the (a) M, (b) T, (c) O1, and (d) O2 phases considered in this study. Hf and O atoms are shown in green and red colors, respectively.

The unknowns in Eq. (1) include the choices of the possible competing phases α, their bulk energies ϵ^{α}, possible surface planes k, and respective surface energies σ_k^{α}. We restrict the value of α to the M, T, and polar O1 and O2 phases (illustrated in Fig. 1). The reasons for these choices are the following: (1) all four phases are competing low energy phases; (2) M and T are the equilibrium bulk phases at room and high (>1973 K) temperatures, respectively, and thin films of hafnia have been reported to crystallize in these phases; (3) O1 or O2 are believed[2,4,6] to be the potential metastable FE phases in hafnia thin films; and (4) the O1 and O2 phases can be easily formed from the T phase owing to low kinetic energy barrier.[6] Further, we consider only low Miller index planes, namely, (100), (010), (001), $(1\bar{1}0)$, (110), (101), and (111) as the possible surface planes (k) due to their expected low surface energies and the natural preference of a material to form low energy surfaces. For the selected subset of phases and surface planes, we require the bulk and surface energies, which we determine using first-principles calculations.

The bulk energies ϵ^{α} of different phases are reproduced from past work[6] in Table I. The surface energies σ_k^{α} of M, T, O1, and O2 phases were calculated using the slab supercells. To ensure comparisons of equivalent surfaces across different phases, equilibrium bulk geometries were reconstructed into supercells with four hafnia formula units such that each phase is easily reducible to T phase by small atomic displacements (as portrayed in Fig. 1).[6] Note that a surface plane, like (100), can have numerous terminations with different stoichiometries, especially for low symmetry phases. It was found that either nonpolar or single oxygen layer stoichiometric terminations are in general the low energy surfaces. Thus, only such terminations were included in this study. Further, hafnia systems with integral number of formula units were only included in this study by considering systems with integral multiples of HfO_2 planes.

Our DFT calculations were performed by using the Vienna *Ab initio* Simulation Package[23] employing the Perdew-Burke-Ernzerhof exchange-correlation functional[24] and the projector-augmented wave methodology.[25] Slabs with aforementioned seven different surface planes were constructed using equivalent supercells discussed earlier with a common vacuum length of 12 Å. A $4 \times 4 \times 1$ Monkhorst-Pack mesh[26] for k-point sampling and an energy cutoff of 500 eV for the plane wave expansion of the wave functions were used. All atoms were allowed to relax until atomic forces were smaller than 10^{-2} eV/Å. Dipole corrections were used to handle the asymmetric nature of some of the surfaces considered, especially in the case of slabs made of polar phases of hafnia. These corrections exclude the spurious energy contributions of dipole-dipole interactions introduced due to the periodic boundary conditions.[27] Certain slabs were transformed to other symmetry phases upon relaxation. Surface energies for such cases were computed by fixing 2–3 hafnia layers in the middle to their bulk like arrangement, thereby avoiding phase transformation. Surface energy of a stoichiometric slab was calculated using the relation $\sigma_k^{\alpha}(t) = \frac{1}{2A_k^{\alpha}}[E^{\alpha}(t) - n\epsilon^{\alpha}]$, where E^{α} is the DFT energy of the slab with thickness t (and σ_k^{α}, A_k^{α} and ϵ^{α} were previously described). Convergence studies of $\sigma_k^{\alpha}(t)$ against slab thickness t was conducted and the converged results are presented in Table I. These were found to be in excellent agreement with available past computational studies. Details of these tests are given in the supplementary material.[28]

Fig. 2 provides a visual comparison of surface energies of hafnia already included in Table I. The T phase displays the lowest surface energy of all surfaces considered except the (001) surface. The phase that showed the lowest (001)

TABLE I. Bulk (ϵ^{α}) and surface (σ_k^{α}) energies of different phases of hafnia. Bulk energies, taken from Ref. 6, are given with respect to the M phase. Surface energies are computed in this work.

	M	T	O1	O2
		Bulk energy (meV/f.u.)		
$\epsilon^{\alpha} - \epsilon^{m}$	0.0	170.6	83.4	142.8
Surface		Surface energy (J/m^2)		
(100)	1.67 (1.67,[21] 1.79[22])	1.55	1.83	2.34
(010)	1.88 (1.88[21])	1.55	2.68	2.34
(001)	1.51 (1.42,[21] 1.45[22])	1.21	1.41	0.79
(110)	1.38 (1.39[21])	1.08	1.98	2.09
$(1\bar{1}0)$	1.38	1.08	1.98	1.69
(101)	1.57 (1.55[21])	1.54	1.61	1.67
(111)	1.25 (1.20,[21] 1.25[22])	1.12	…	…

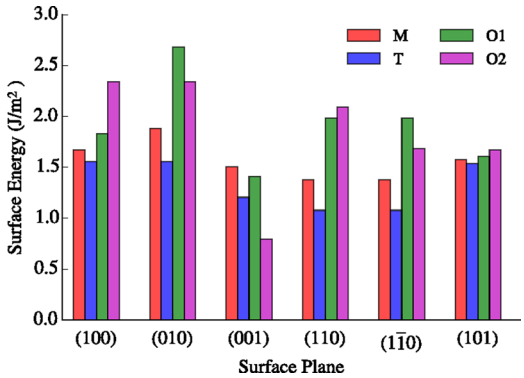

FIG. 2. Surface energies corresponding to different orientations computed for the M, T, O1, and O2 phases of hafnia.

surface energy is O2. These points become relevant later when applying Eq. (1) for the 4 hafnia phases. Interestingly, both the polar phases have lower (001) surface energies than that of the equilibrium M phase. Thus, metastable phases, especially polar phases decorated with (001) surface planes, can have lower overall energy than that of the M phase when surface energy contributions are substantial. Due to the difficulties encountered in achieving converged (111) surface energies for polar phases and the small differences between the (101) surface energies across the studied phases, the (111) and (101) surfaces were excluded in subsequent steps.

Once all variables in Eq. (1) are known, the model can be used to predict the energetic ordering of different phases of hafnia within the particle model. First, we apply our model to the case of 2D slabs, a special case of the particle model. This allows us to not only validate the limiting behavior of our model against first-principles calculations but also explore the role of increasing surface-to-volume ratio. Fig. 3 presents the relative stability ordering of slabs of different hafnia phases as a function of the inverse of the slab thickness t. Interestingly, the metastable T and O2 phases appear to be stable at very short length scales ($\lesssim$25 Å) for certain slab orientations. The DFT slab calculation results are also included in the Fig. 3. They can be seen to converge to the corresponding slab model energy lines, illustrating the correspondence between the converged DFT surface energies and the results of the particle model. At extremely small slab thickness, however, there exist minor deviations in the model predicted and the DFT computed energies due to the difference in the converged surface energy used by the model and the actual surface energy computed using DFT. For certain stoichiometric slabs, multiple types of surface terminations, each with its associated surface energy, were possible. For example, the (001) slab of the O2 phase has two different surface energies corresponding to

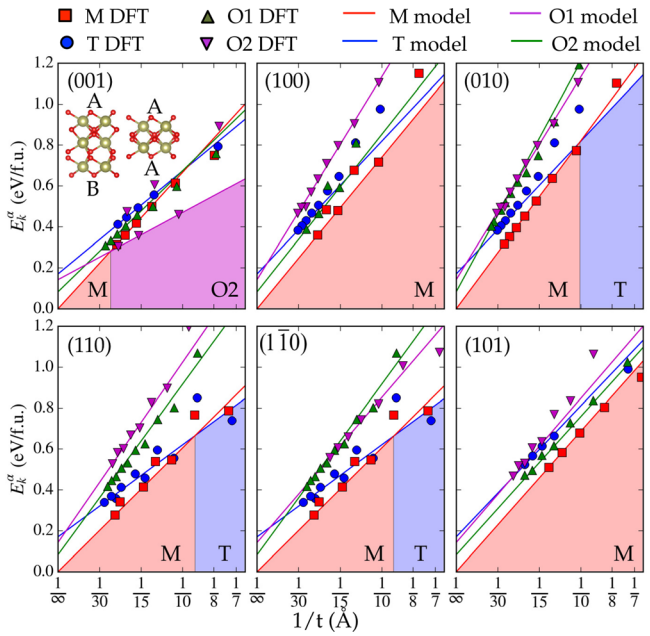

FIG. 3. DFT-based and model-predicted (via Eq. (1)) energy of (001), (100), (010), (110), (1$\bar{1}$0), and (101) hafnia slabs referenced to the energy of the bulk M phase. The inset displays two types, marked A and B, of the (001) surfaces of the O2 phase.

the two types of surface terminations (see inset in Fig. 3). In such cases, surface planes with least energy were selected to construct stability diagrams discussed later. This, however, implies a limitation to the model, i.e., the model cannot account for multiple types of terminations of the same surface but only for the lowest-energy one. In the limit of $t \to \infty$, the slab reduces to a bulk system and the surface contributions vanish. This is captured by the slab model energy lines as they approach the corresponding bulk energies (given in Table I) when $1/t$ approaches zero. Although the length scale for stabilizing the metastable phases in slabs is extremely small, it can be expected to be substantial in lower dimensional models where the surface-to-volume ratio is higher.

Next, we apply our model to hafnia particles terminated by (100), (010), and (001) sidewalls. Based on Eq. (1), we plot the stability diagrams as a function of the parallelepiped dimensions in Fig. 4. Similar to slabs, both the T and O2 phases appear to be stable at short length scales. At small [100] lengths, the energy contributions from the (010) and (001) surface area dominates and the T phase is stabilized. However, at extremely large [010] lengths, only the (001) surface contribution dominates and the O2 phase with lowest (001) surface energy is stabilized. Further, the M phase, with least bulk energy, appears in the phase diagram at significant

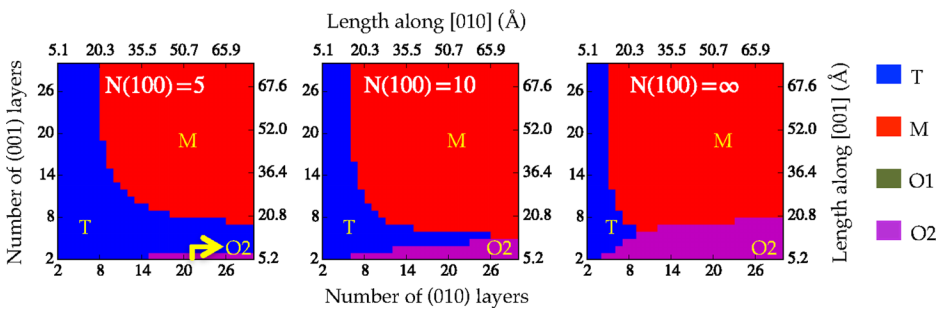

FIG. 4. Stability diagrams of a hafnia particle terminated by (100), (010), and (001) surfaces based on Eq. (1) at different [100] dimensions. Here, N(100) represents the number of (100) planes while the length along the [001] and [010] directions of the T phase are shown in the top and the right axes, respectively.

[010] and [001] lengths where the volume contribution dominates. As length along [100] increases (Figs. 4(b) and 4(c)), contributions from (001) surface area increases and the region where the O2 phase stabilizes expands. When [100] approaches infinity, the 0D particle reduces to a 1D rod. Fig. 4(c), thus, represents the stability diagram of a hafnia rod with [100] axis and (010) and (001) surfaces.

Although results for one special (100)–(010)–(001) hafnia particle were presented here, similar trends of stabilization of the T and O2 phases were obtained with other surface combinations (included in the supplementary material).[28] This is expected since the T surface energies are consistently lower than that of the reference M phase for all surface planes considered and because the O2 phase has the least (001) surface energy. Our results are consistent with several experimental observations of the T phase in ultrathin hafnia films and nanotubes,[9] and match well with the critical grain size of 4 nm for the stabilization of the T over the M phase.

Although our model suggests stabilization of the T and O2 phases in hafnia particle of small dimensions, this conclusion cannot be directly extended to polycrystalline hafnia films which have interfaces rather than free surfaces. However, if the fair approximation of equivalence of interface and surface energies is made, two pathways for the stabilization of FE phases can be expected using our model: (1) stabilization of the O2 phase due to (001) surface planes or (2) stabilization of the T phase followed by transformation to either of the O1 or O2 phases due to other perturbations (e.g., strain, electric field).[6] Empirical observations, nevertheless, indicate stabilization of the FE O1 phase in hafnia films. Difference between our conclusions (purely based on strain-free bulk and surface energy considerations) and the empirical observations should be accounted for in the future by including other key factors such as strain, interfaces, impurities/dopants, etc., presently omitted.

Finally, we note that the conceptual learning from this study can be extended to pure zirconia systems where stabilization of the metastable T phase, instead of the equilibrium M phase, is believed to occur due to surface energy effects.[10] A similar strategy can be adopted to estimate the length scales up to which the T phase can be stabilized in zirconia systems, although, given the similarity of hafnia and zirconia, one can expect present conclusions to be directly applicable to zirconia as well.

In summary, we have studied the possible surface-induced stabilization of metastable phases in pure hafnia by first-principles computations. We find that at nano length scales, surface energies can stabilize either the polar O2 phase or the tetragonal phase, which, in turn, can transform into the polar O1 or O2 phase. This provides a possible explanation of the FE behavior observed in pure hafnia films reported in Ref. 12, although other relevant factors need to be further included to arrive at a comprehensive understanding of this phenomenon. The general computational scheme presented in this work can be used to study the stability of metastable phases in other materials due to the surface effects. Indeed, our results can be immediately extended to explain the occurrence of the metastable tetragonal phase in nano-powders of zirconia, which is structurally and chemically similar to hafnia.

Financial support of this work through Grant No. W911NF-15-1-0593 from the Army Research Office (ARO) and partial computational support through a Extreme Science and Engineering Discovery Environment (XSEDE) Allocation No. TG-DMR080058N are acknowledged.

[1]T. S. Böscke, J. Müller, D. Bräuhaus, U. Schröder, and U. Böttger, Appl. Phys. Lett. **99**, 102903 (2011).
[2]M. H. Park, Y. H. Lee, H. J. Kim, Y. J. Kim, T. Moon, K. D. Kim, J. Müller, A. Kersch, U. Schroeder, T. Mikolajick, and C. S. Hwang, Adv. Mater. **27**, 1811 (2015).
[3]O. Ohtaka, H. Fukui, T. Kunisada, T. Fujisawa, K. Funakoshi, W. Utsumi, T. Irifune, K. Kuroda, and T. Kikegawa, J. Am. Ceram. Soc. **84**, 1369 (2001).
[4]X. Sang, E. D. Grimley, T. Schenk, U. Schroeder, and J. M. LeBeau, Appl. Phys. Lett. **106**, 162905 (2015).
[5]S. Mueller, J. Mueller, A. Singh, S. Riedel, J. Sundqvist, U. Schroeder, and T. Mikolajick, Adv. Funct. Mater **22**, 2412 (2012).
[6]T. D. Huan, V. Sharma, G. A. Rossetti, and R. Ramprasad, Phys. Rev. B **90**, 064111 (2014).
[7]S. E. Reyes-Lillo, K. F. Garrity, and K. M. Rabe, Phys. Rev. B **90**, 140103 (2014).
[8]J. E. Lowther, J. K. Dewhurst, J. M. Leger, and J. Haines, Phys. Rev. B **60**, 14485 (1999).
[9]M. Shandalov and P. C. McIntyre, J. Appl. Phys. **106**, 084322 (2009).
[10]J. Chevalier, L. Gremillard, A. V. Virkar, and D. R. Clarke, J. Am. Ceram. Soc. **92**, 1901 (2009).
[11]R. Materlik, C. Künneth, and A. Kersch, J. Appl. Phys. **117**, 134109 (2015).
[12]P. Polakowski and J. Müller, Appl. Phys. Lett. **106**, 232905 (2015).
[13]M. Hyuk Park, H. Joon Kim, Y. Jin Kim, T. Moon, and C. Seong Hwang, Appl. Phys. Lett. **104**, 072901 (2014).
[14]C. M. Fancher, L. Zhao, M. Nelson, L. Bai, G. Shen, and J. L. Jones, J. Appl. Phys. **117**, 234102 (2015).
[15]U. Schroeder, E. Yurchuk, J. Müller, D. Martin, T. Schenk, P. Polakowski, C. Adelmann, M. I. Popovici, S. V. Kalinin, and T. Mikolajick, Jpn. J. Appl. Phys., Part 1 **53**, 08LE02 (2014).
[16]C.-K. Lee, E. Cho, H.-S. Lee, C. Hwang, and S. Han, Phys. Rev. B **78**, 012102 (2008).
[17]D. Hou, C. M. Fancher, L. Zhao, G. Esteves, and J. L. Jones, J. Appl. Phys. **117**, 244103 (2015).
[18]M. W. Pitcher, S. V. Ushakov, A. Navrotsky, B. F. Woodfield, G. Li, J. Boerio-Goates, and B. M. Tissue, J. Am. Ceram. Soc. **88**, 160 (2005).
[19]P. Hohenberg and W. Kohn, Phys. Rev. **136**, B864 (1964).
[20]W. Kohn and L. Sham, Phys. Rev. **140**, A1133 (1965).
[21]A. B. Mukhopadhyay, J. F. Sanz, and C. B. Musgrave, Phys. Rev. B **73**, 115330 (2006).
[22]X. Luo, A. Demkov, D. Triyoso, P. Fejes, R. Gregory, and S. Zollner, Phys. Rev. B **78**, 245314 (2008).
[23]G. Kresse and J. Furthmüller, Phys. Rev. B **54**, 11169 (1996).
[24]J. P. Perdew, K. Burke, and M. Ernzerhof, Phys. Rev. Lett. **77**, 3865 (1996).
[25]P. E. Blöchl, Phys. Rev. B **50**, 17953 (1994).
[26]H. J. Monkhorst and J. D. Pack, Phys. Rev. B **13**, 5188 (1976).
[27]G. Makov and M. C. Payne, Phys. Rev. B **51**, 4014 (1995).
[28]See supplementary material at http://dx.doi.org/10.1063/1.4947490 for (A) surface energy convergence study, (B) Stability diagram of (110), (1$\bar{1}$0) and (001) hafnia particle.